Response to reviewer #1:

We thank the reviewer for very helpful comments that made it possible for us to improve the manuscript. Point-by-point responses to the reviewer's comments are given below; the original comments are included in italics. All changes in the revised manuscript is marked in bold.

General comments
Carlson and Caballero address an important and relevant question: Could changes in cloud properties have contributed to Eocene warming, in ways that might be reflected in the proxy record? The paper focuses on analyzing a new simulation where changes in cloud radiative properties are altered from a more conventional Eocene forcing scenario, and a smaller greenhouse gas forcing is needed to achieve the same change in global-mean temperature change.

The paper makes an interesting contribution to the literature. The question and analysis are well within the scope of Climate of the Past. The abstract provides a concise and complete summary. The authors thoroughly reference existing literature and appropriately highlight their contribution. The presentation is well-structured and clear, as is the language, and the wording is sufficiently precise.

The paper shows that the greenhouse-gas and cloud driven mechanisms of Eocene warming have similar temperature changes (both of which are consistent with the proxy record), but differ in their hydroclimate and circulation changes. The implication is that proxies of circulation and hydroclimate would be able to differentiate between these two forcing mechanisms. The case for how hydroclimate and circulation proxies could differentiate the two warming scenarios is not completely clear-cut. In addition to the caveats already addressed in the concluding section, another important caveat is that this study is based on only one model. Different climate models have different biases, which are often larger for hydroclimate and circulation than they are for temperature. Also, the changes in cloud effective radius employed here are probably too large to be realistic (according to the discussion of Kiehl and Shields 2013). Another concerning feature of the simulation is that the radiative properties of clouds are altered but the microphysical properties are not, so in a sense the simulation is not completely self-consistent. This is particularly important because the conclusions are largely focused on hydroclimate, which might be affected by changes in microphysical properties of clouds. This lack of change in cloud microphysics is not described in the methods section (where it should be mentioned), it is discussed extensively in the conclusions.

Ans: This is an important caveat and it should be clear in the description of the simulations. We have now mentioned it in the methods section in the revised manuscript.

In light of the implications for differentiating forcing mechanisms from the proxy record, a more extensive discussion of potential proxy records for regional climate and hydroclimate would be warranted (the beginnings of a discussion is included at the end of section 6). Is there existing relevant proxy evidence? Are there existing methods with which new records might be identified in new locations, or would new reconstruction methods need to be developed? Is it likely that useful records could be

found over land, and if so in which regions? Or would useful records need to be identified in the ocean?

Ans: While we agree that a more comprehensive discussion of the extant and potential new proxies would be of great interest, we prefer not to delve too deeply in that direction here as it lies beyond our area of core expertise, which is in physical climate dynamics. Our goal here is simply to make a *prima facie* case from the climate dynamics perspective that the approach taken here could be a fruitful line of future, more detailed work, involving also the proxy community. We have added some lines in the Introduction to better clarify the aim and scope of our work.

The title of the paper could be improved in two very minor ways. The first is that the analysis focuses on just one alternative mechanism for Eocene warming, but the title implies there are multiple. Second, hydroclimate seems to be a bigger focus than circulation, and is also is a more likely candidate for the focus of new proxy evidence than circulation. The order of the terms might be switched to reflect this.

Ans: In response to comments from Reviewer 2, who convincingly argued for the potentially misleading nature of our approach to terrestrial hydroclimate, we have opted to remove that section (Section 6 in the original manuscript) from the paper. We feel that the climate dynamics-oriented material in Sections 4 and 5 is sufficiently extensive and novel to justify publication. We have also added a new figure and a substantial amount of new text to Section 3 dealing with seasonal and diurnal temperature ranges, which will be of interest to the proxy community. Given this refocusing, we feel that the paper's title adequately describes its contents.

The quality of the figures is generally adequate. Given the focus, it would be useful to see absolute fields for things like precipitation and aridity in the LCTC simulation, rather than just their differences from the Control case. This could be accomplished by showing the LCTC absolute fields rather than the control fields, but it would also be useful to have both in addition to the differences. Some of these could be included as a supplement. If one figure were to be omitted, I would suggest Figure 6. Its discussion is already limited in the text. In Figure 7, the caption states that fields are shown over land only, but panels a and c seem to have some faint signal over the ocean; it would be worth removing this, otherwise it gives the impression that changes over ocean are included and are uniform but small.

Ans: Thank you for pointing this out. We have included the absolute fields for the LCTC scenario in the supplementary material. The Figure 7 comment is no longer relevant since it has been excluded in the revised manuscript, see response to referee 2.

Specific comments
Page 3 Line 3: A more descriptive name than "control" might be devised for the greenhouse-gas driven Eocene scenario. More descriptive names for both scenarios might be "GHG" and "Cloud."

Ans: This is a good suggestion. We have changed the name of the control run to GHG but kept the name LCTC for the scenario with increased cloud droplet radius.

Line 4-5: Rather than cloud droplet radius, the relevant variables is the effective cloud droplet radius. It represents a weighted average over the distribution of cloud droplets.

Ans: This is an important distinction and it is corrected in the revised manuscript.

Page 4 Line 5-8: Just how similar is the temperature for the two simulations? You might quantify this as the maximum difference in zonal-mean temperature. Figure 2b makes it seem like they could be non-trivial.

Ans: The maximum difference between the GHG and LCTC zonal-mean temperatures is 0.93 K, we have added this to the text referring to Fig. 1. (Please note that lines 5-8 in page 4 of the original manuscript referred to a comparison between our GHG simulation and previously published (Huber and Caballero 2011) simulations with a coupled climate model under the same conditions; however, given the reference to Fig. 2b, we believe the reviewer is referring to the difference between the GHG and LCTC runs).

Page 5 Line 10-15: The jet streams vary among climate models and between models and observations in the present-day climate, and these variations are related to changes in the jet with climate (see Barnes and Polvani 2013 for the differences across models). The appropriate comparison with present-day jet streams would be to CAM3 with modern boundary conditions and forcings, whereas Shaw et al (2016) focus on reanalysis data.

Ans: This is a good point and we have added a reference that specifically looks at the jet streams in modern-day CAM3 (Hurrell et al. 2006), which shows that the modern zonal orientation of the Pacific jet is well represented in CAM3. We have elected to keep the reference of Shaw et al 2016 as well.

Line 21: Caution should be exercised in interpreting the MJO in coarse resolution climate models. There are many aspects of it that they are not able to represent with particularly good fidelity (e.g. Hung et al 2013).

Ans: This is a good point and in fact for a cold climate the model used here, CAM3, has very weak MJO-like variability. However, as is discussed in Carlson and Caballero 2016 in a warmer climate the tropical subseasonal variability is increasingly MJO-like. Although Carlson and Caballero 2016 looked at an aquaplanet ,a similar increase is seen in an Eocene configuration as was shown in Caballero and Huber 2012.

Page 6 Line 19-23: It seems to me that 6 out of 17 Wmˆ-2 contributed by changes in cloud radiative effect is an important fraction of the total change in atmospheric radiative cooling.

Ans: We agree and have qualified the statement with "makes a substantial contribution".

Line 23: Rather than "cloud abundance," the cloud radiative effect might change due to the changes in cloud properties that are specified (effective cloud droplet radius).

Ans: Yes, it is true that changes in LW cloud emissivity due to changed droplet size could also contribute to changes in cooling, and we have added this to the text.

Page 8 Line 6-7: Why is Fig 5d noisier than Fig 2d?

Ans: Through using the tool of a fixed SST model we have attempted to isolate the effect of the three different mechanisms. However, it is expected that the results are slightly different when comparing the full run (Figure 2d) and the linear sum of the three fixed SST runs (Figure 5d). The fact that the results are so similar is a motivation that the change we see is mainly due to these three effects, this conclusion is qualitative and based on the large scale similarity of Figure 2d and Figure 5d. The fact that the precipitation in the individual runs is not as noisy as the sum could suggest that the noise is an artifact of simply taking a linear sum.

Minor comments

Page 4 Lines 5,12: Figures 1 and 2 are shown in a different order from their reference in the text.
Line 22: "cyclones" should be "anticyclones"
Line 25: "essentially identical" is difficult to quantify, "very similar" might be more defensible
Page 5 Line 5: "cloud abundance" should be "cloud fraction"
Page 12 Line 24-26: The reference information for Carmichael et al (2015) seems to be out of date. The final published version of the paper came out in 2016 and has a different title.

Ans: All of the minor comments above are very useful and have been addressed in the revised manuscript according to the suggestions above.

Figure 3: I expected each color to balance across each panel, but they do not. The figure presentation might be a little bit clearer.

Ans: This is a good point and it needed clarification. We have changed Figure 3 in order to make it clearer.

Response to reviewer #2:

We thank the reviewer for very helpful comments that made it possible for us to improve the manuscript. Point-by-point responses to the reviewer's comments are given below; the original comments are included in italics. All changes in the revised manuscript is marked in bold.

This study uses a global climate model to try to answer the very interesting question of how warm worlds due to CO2 are different from warm worlds due to shortwave forcing (represented here by reduced cloud albedo), and how we might be able to see the difference in the geologic record. It is a fascinating and wide-ranging paper with a lot of insight.

However, on one key point (how to leverage the paleovegetation record) I think it is really missing the forest for the trees, so to speak. Namely, it focuses on regional water-induced vegetation differences between the two scenarios using a metric that the authors admit may not have much relevance. Yet direct CO2-induced vegetation differences would probably be much more one-sided, larger and easier to detect (and by my reading of the literature would be likely to overwhelm the water-induced differences, calling their highlighting here into question.) Thus I recommend major revisions before full publication. I also have quite a few more minor science suggestions and writing suggestions under Minor afterward.

Major issue:
*p2 li22, p9 li7-10, etc: The vegetation patterns might indeed carry some signature of the different hydrological cycle or regime, but an even stronger vegetation signature of LCTC vs. high-CO2 would be the direct CO2 effect on the vegetation itself! One would expect a very-high-CO2 world to be much greener than today's, with plants surviving in hydroclimate regimes that today cannot support them (because of the much lower transpiration losses in order to fix a given amount of CO2, i.e. the increased water-use efficiency.) In contrast, an LCTC world would not be expected to be particularly greener or browner than today's, except where induced by regional hydroclimate change. So the global vegetation extent and pattern could be a key *direct* indicator of the mix of forcings, independent of the forcings' effect on the water cycle. Certainly the vegetation pattern you prescribe (from the figure in Sewall et al 2000) is much greener than today's, with no unvegetated or desert-vegetation areas and very extensive forests, so you are almost implicitly assuming a major role for CO2 (or at least Sewall did.)*

Similarly at end of page 3 and beginning of page 4 (and again p9 li12-13), yes the high CO2 might change the stomatal conductance and thus the terrestrial hydrology, but even more importantly it would dramatically change the vegetation itself (which is the thing you want to observe in the geologic record as you say on p9 li8-9), even before you get to the hydrology (!) You allude to this at p9 li13-14 when you cite the Roderick paper, but the way you put it is quite an understatement. Far from just "imperfect", the P/PET seems to have essentially nothing to do with the vegetation response when CO2 changes are involved: : : the CO2 utterly dominates. At least in models. See the plot in the Scheff manuscript, it is pretty stark (and largely backed up by the paleo vegetation data as they discuss.)

So I would strongly suggest getting rid of the whole PET-based analysis and instead looking at the land model's direct photosynthesis and/or leaf-area-index output if you want something you can qualitatively compare to paleovegetation records. Again, the contrast between the high-CO2 (fertilized) and the LCTC (unfertilized) case should be dramatic to say the least, unless the land model you are using is so old that it doesn't include CO2 effects. If you do this, you should add "and global vegetation" after "regional climates" at p11 li14.

*I see that you are aware of this to some degree, and trying to get at this with the caveats and narrowing of the scope at p9 li21-24 and p10 li3-7 & li26-29. But it would seem cleaner and more of a clear demonstration to just plot the simulated changes in vegetation quantities like photosynthesis or LAI, instead of qualitatively fudging together the P/PET index changes with a vague expectation of additional greening/browning. It would also better highlight the most useful way of distinguishing high-CO2 from LCTC in the paleovegetation record - via the *direct* CO2 effects which have potentially global scope, rather than via the water effects which are much more regional and iffy as you point out.*

Note, you can still keep all the precipitation and circulation stuff, since precipitation will still be relevant for understanding changes in P-E which will manifest themselves inproxies like paleo rivers and lakes, signatures of soil infiltration rates, etc. Precipitation also directly drives some of the paleomagnetic proxies. So I'm just talking about replacing sections 6 and 2.2 here, not touching the bulk of the paper which is much more relevant.

If you are really after differences in "eco-hydrological regime" (p9 li15) rather than vegetation per se, then I'd strongly recommend using P/Rnet (as suggested by the Milly and Dunne paper) rather than P/PET, to be conservative. But I'm not sure this is the best approach either, since there is no paleoproxy for eco-hydrological "regime" whatever that is. Instead there are proxies for specific tangible things like vegetation, rivers, lakes, infiltration rates, water isotopes, paleomag, etc. that all respond quite differently to global climate change. In particular, vegetation responds very differently from P/Rnet or P/PET when CO2 is involved (as far as we can tell.) Another way to see this is that satellite data shows the Earth is greening in recent decades (Zhu et al. 2016 Nature Climate Change) even while a P/PET calculation would tell you it has been drying (some of Fu's papers which analyzed historical data). This implies P/PET is not just "imperfect" for vegetation change under CO2/climate change, but grossly misleading.

Ans: Thank you for making such a thorough and constructive comment. We were aware that the usefulness of P/PET is limited and as you say we tried to get some qualitative understanding of the problem using this rather blunt tool. However, we agree that relying solely on P/PET risks giving a biased and potentially misleading perspective on our results. We have therefore decided to exclude Section 2.2 and Section 6 based on your comment and the references in it.

Replacing it with direct output from the land model is a good suggestion, but when looking further into this issue, we realized that the land model that we used, CLM2, has CO2 concentration hardcoded in the model and the vegetation will not be affected by changes in CO2 concentration specified for the atmosphere. This means that

stomatal conductance will not be affected by the change in CO2 between the two simulations, biasing the transpiration and P–E values. We have therefore decided not to address terrestrial hydroclimate, refocusing the manuscript towards the precipitation and circulation parts. We have taken up some of the space freed up by adding a new figure and discussion of seasonal and diurnal temperature ranges, in response to your suggestion below. We feel that the resulting manuscript is more solid and defensible, and contains sufficient substance and novelty to warrant publication.

Minor: (Note, some of these are on the PET parts, so they will not be relevant if you decide to replace the PET analysis as suggested above.)

*p1 li10: Do you mean 11% greater absolute precip, or 11% larger precip *response* to warming? This should be clarified. See p4 li26-29 comment below.*

Ans: We mean that global-mean precipitation in LCTC is 11% greater than in the GHG case. We have clarified this in the abstract and also in the relevant section of page 4, see below.

pi li24-25: Can you at least include a few words about why one might think the Eocene would have fewer aerosols than the present? I.e., does this hypothesis just come out of nowhere or is there some qualitative speculation/cartoon behind it? Given how vegetated and warm the Eocene was, I would a priori think it would have more aerosols than present, via much-increased biogenic VOC emissions as well as more fires (more fuel.) Though, I suppose it would also have less dust due to the increased vegetation cover. So it could go either way.

Ans: We have added some additional background and references in the introduction to motivate this assumption, though we emphasize that it remains highly speculative. It is precisely the uncertainty in Eocene aerosol/cloud forcing that serves as the main motivation for this paper.

p2 li30-31: The atmosphere and ocean models are specified here, but not the land model. What land model was used?

Ans: The land model used in the simulations was CLM2. That should have been included in the model description. Thank you for pointing this out and we have addressed it in the revised manuscript.

*p2 li32: By prescribing a seasonally-varying q-flux but *also* using a slab mixed-layer ocean, you may be double-counting the seasonal storage and release of heat in the mixed layer: : : be careful here. What is the depth of the slab ocean? If you are going to use a seasonally-varying q-flux, your slab ocean should probably have minimal depth, since the seasonal cycle of the q-flux is *already* dominated by the fluxes in and out of the ocean every year due to seasonal warming and cooling of the mixed layer. (Does this make sense?) In this case, you should also insert "and seasonal storage" after "transport" on line 31.*

Ans: That is a good point. The qflux used is indeed seasonally varying, and the slab has 50 m uniform depth (this detail has been added in the Methods section). While the annual-mean temperature is in good agreement with the coupled model simulation of

Huber and Caballero (2011) (~2C differences in the zonal- and annual mean), there are larger seasonal differences, which makes the mid/high latitude annual temperature range in both hemispheres of our GHG simulation about 5C smaller than in the coupled model. There is no easy way around this problem. The qflux is determined from the climatological monthly-mean net surface heat flux in the coupled model, which—as the reviewer correctly points out—includes a storage term. The storage term is negligible in the annual mean, but specifying a time-invariant annual-mean qflux would also lead to bias since ocean heat transport does have a seasonal variability. However, determining the actual seasonally-varying ocean heat transport would involve computing it from the 3-dimensional ocean current and temperature fields in the coupled model, to which we do not have access. In any event, our paper focuses on comparing two simulations run with the same qflux, so we believe that our results will be at least qualitatively robust to different specifications of this qflux. We have added some more text in the methods section discussing this issue.

p3 li25: For the reader unfamiliar with hydrology and PET, you should also mention that capital Delta is the slope des/dT of the es curve (instead of just giving its numerical formula out of context.)

Ans: This is a good suggestion but it is no longer relevant since we have excluded the P/PET part of the paper.

p3 li29-32: Scheff and Frierson (2015, the follow up to the 2014 paper) checked the monthly assumption more closely. They found that it's not bad at all for changes in PET (probably because the day-night warming difference isn't actually that big in most places) though it can throw off the absolute PET values by double-digit percentages. However, they only tested greenhouse-driven warming, so I don't know if the result would be valid for LCTC/shortwave warming. Presumably the LCTC world warms much more during the day than at night, so this time-resolution issue could actually become important. In fact, the diurnal cycle of temperature could be another major constraint detectable in the paleoecological record - plant species composition may respond quite differently to warming with much-increased diurnal cycle (LCTC) than warming with unchanged or somewhat reduced diurnal cycle (CO2) because different species have different tolerances to min and max temperature. Again this would be independent of any watercycle- driven vegetation change. Thus, it would be interesting for you to quantify the difference in diurnal Tmax and/or diurnal Tmin between your two Eocene end-members, not just the difference in Tmean. Either of these may be quite dramatic, even though the Tmean doesn't differ much. All of this may additionally hold for seasonal cycle (winter and summer temperatures rather than annual-mean temperature.) We have a good idea of winter temperatures from some of the proxies like crocodiles and palm trees surviving in the Arctic. Some SST proxies are also particularly sensitive to summer temperature so they could be useful here.

Ans: This is an excellent suggestion, and we have added a new figure (Fig 3 in the revised manuscript) as well as 3 new paragraphs of text in Section 3 discussion changes in seasonal and diurnal temperature ranges.

General:
The first mention of Figure 1 right now (p4 li12) comes after the first mention of

Figure 2 (p4 li5). So these two figures should be reversed and re-numbered accordingly. I.e. you need to re-number the current Figure 2 as Figure 1, and vice versa.

Ans: The two figures in question have been renumbered in the revised manuscript.

p4 li26-29: Not only is it a substantial increase due to this reasoning, it's also a substantial increase because it's on the same order or larger than what you would get by differencing LCTC with a Holocene run (or differencing high-CO2 with a Holocene run.) In general it might be more useful to contrast the differences of high-CO2 and LCTC with a common Holocene-like (i.e. low-CO2, normal-cloud) control, instead of contrasting the absolute precip values. I.e. by what factor or percentage is the LCTC-Holocene difference larger than the highCO2-Holocene difference. It will be a lot more than 11%. And it's that difference from present that we tend to notice when we think about Earth system change over time, not the absolute value.

Ans: The precipitation increase from modern to GHG is actually about twice as large as the increase from GHG to LCTC, in agreement with the precipitation scaling implied by the Carmichael et al paper. We have added some text in page 4 to point this out. We agree that including a comparison of both GHG and LCTC cases with a modern preindustrial run would be of interest, but to do such a comparison justice would require a large number of additional figures and a lot more analysis and text. We have added references to papers providing extensive information on modern CAM3 simulations (Hurrell et al. 2006, Collins et al. 2006) that the interested reader may consult.

p4 li29-34: This needs to cite Fig 2d.

Ans: We have added the citation in the revised manuscript.

p5 li3-4: No it doesn't "only" prescribe change in cloud droplet size - it also prescribes a big change in CO2 (of course.) The effects of the CO2 difference could also be important for the big cloud cover changes you see. Again, differencing both simulations with a common low-CO2 normal-cloud control would help in disentangling this.

Ans: Yes, that is of course true; we meant that the only cloud property directly modified in the LCTC case is droplet size. We have modified the sentence in question to include the change in CO2. The issue of disentangling the separate effects of droplet size and CO2 is addressed by the fixed SST runs, in which these parameters are changed one at a time (which is a cleaner solution, since a modern simulation would have different geography and land cover, adding confusion).

p5 li10: Not to sound like a broken record here, but does a "modern" (Holocene-like) control simulation with this model also have this Pacific meridional tilt? You may just be seeing a general bias of the model, not a particular effect of the Eocene climate. Exact same issue with "than observed in the modern climate" at li14-15, too. If Eocene model is different from modern observation, it's hard to tell whether that difference is due to "Eocene vs. modern" or whether it's due to "model vs.

observation" (without further information or citations.)

Ans: No, as shown in Hurrell et al. 2006, a modern simulation with CAM3 captures the Pacific jet quite well (and does not have the large meridional tilt seen in our GHG simulation). We have added this reference and some additional text to clarify this point.

p6 li1: Strictly speaking this equation will give a negative value for P, since LH as you just defined it will be a negative number (LH is upward, not downward) while Lv is positive. So you may want a minus sign in this equation to be technically correct.

Ans: This is correct and we have added a minus sign in the revised manuscript.

p6 li8 and Fig 3: It's not immediately clear what bars in Figure 3 to look at to see "Atmospheric heating". It seems for SW and LW it's the black (TOA-surface) bar, but for LH and SH it's actually the orange (surface) bar. So this would be easier to read if you made black bars for LH and SH as well, and explicitly pointed out in the text or the figure caption that the black (TOA-surface) is the (net) atmospheric heating in all cases. In this case you would also flip all of the orange bars to opposite sign, to be consistent with your definition of negative up, positive down (see previous comment.) Then, the coloring would be consistent across all four heat transfer mechanisms. Alternatively you could keep your opposite-sign convention for the orange bars, but then you should rename the black bars to "atmospheric heating" rather than TOA minus surface, since strictly speaking they are TOA plus surface in the current graphical setup.

Ans: This was unclear in the manuscript and we have changed Figure 3 to make it consistent according with the first suggestion above. In addition, we added a clarification in the caption that the black bars are the atmospheric heating.

Also p6 li8: it's hardly "dominated" by the LH component, the SW component is actually almost as big! Rather you could just say that LH is the largest component (a lot more defensible.) "Dominated" means much larger than the others, not just larger.

Ans: This is a good point, we have changed the text accordingly in the revised manuscript.

p8 li4: I assume this is supposed to be "westerly anomaly" (i.e. east-pointing.)

Ans: It is corrected in the revised manuscript to westerly anomaly.

p9 li17-18: This should have a citation (e.g. to Middleton and Thomas) so the reader can know who is doing the classifying.

Ans: This is not relevant in the revised manuscript.

p9 li19-20: Low relative humidity is also very important for this, I think (you could check
this.)

Ans: This is not relevant in the revised manuscript.

p10 li27: As alluded in the major comment, "eco-hydrological differences" is too vague because plants, rivers, soils, precip, etc. all respond to CO2-driven climate change in such a different manner from one another. If you mean vegetation, just say vegetation. (If you mean something else, say something else.)

Ans: This is not relevant in the revised manuscript.

Figures 7a and 2c: It's hard to see the precipitation patterns over most of the planet, because most of the map is in the very light colors which don't distinguish from each other easily. You may want to have your color scales saturate to dark at lower precipitation values (e.g. 9 instead of 18) to make the patterns easier to see. More than 9 mm/day is very wet by anyone's measure.

Ans: Figure 7a is excluded in the revised manuscript. See answer to the major issue above. It is a good suggestion and makes Figure 2c much more informative.

Figures 7a and 7c: Color values still seem to be plotted over the ocean, even though you are not trying to plot ocean points. This is a little confusing, and for 7a it worsens the above problem. Make sure the oceans are actually white here (or some other neutral color.)

Ans: Figure 7a and 7c is excluded in the revised manuscript See answer to the major issue above.

Typos:
p2 li30: "research" needs to be capitalized in the name of NCAR.
p4 li22: should be "subtropical anticyclones" rather than "subtropical cyclones" (I presume?)
p5 li9: "zonal winds are in the Northern Hemisphere: : : are concentrated" should be "zonal winds in the Northern Hemisphere: : : are concentrated"
p8 li14: extra word "may" near the beginning of this line

Ans: All the above typos have been addressed in the revised manuscript

Atmospheric circulation and hydroclimate impacts of alternative warming scenarios for the Eocene

Henrik Carlson[1] and Rodrigo Caballero[1]

[1]Department of Meteorology and Bolin Centre for Climate Research, Stockholm University

Correspondence to: Henrik Carlson (henrik@misu.su.se)

Abstract. Recent work in modelling the warm climates of the Early Eocene shows that it is possible to obtain a reasonable global match between model surface temperature and proxy reconstructions, but only by using extremely high atmospheric CO_2 concentrations or more modest CO_2 levels complemented by a reduction in global cloud albedo. Understanding the mix of radiative forcing that gave rise to Eocene warmth has important implications for constraining Earth's climate sensitivity, but progress in this direction is hampered by the lack of direct proxy constraints on cloud properties. Here, we explore the potential for distinguishing among different radiative forcing scenarios via their impact on regional climate changes. We do this by comparing climate model simulations of two end-member scenarios: one in which the climate is warmed entirely by CO_2 **(which we refer to as the GHG scenario)**, and another in which it is warmed entirely by reduced cloud albedo (which we refer to as the "low CO_2-thin clouds" or LCTC scenario) . The two simulations have almost identical global-mean surface temperature and equator-to-pole temperature difference, but the LCTC scenario has $\sim$11% greater global-mean precipitation **than the GHG scenario**. The LCTC **scenario** also has cooler midlatitude continents and warmer oceans than the **GHG** scenario, and a tropical climate which is significantly more El Niño-like. **Extremely high warm-season temperatures in the subtropics are mitigated in the LCTC scenario, while cool season temperatures are lower at all latitudes. These changes appear large enough to motivate further, more detailed study using other climate models and a more realistic set of modelling assumptions.**

1 Introduction

The Early Eocene ($\sim$50 Ma) was characterized by very warm surface temperatures compared with the present day (Huber, 2008; Pagani et al., 2014). Considerable progress has been made recently in reconciling proxy temperature reconstructions with climate model simulations of this period: models can now capture both the reconstructed global-mean and equator-pole temperature difference with much greater fidelity than before (Huber and Caballero, 2011; Lunt et al., 2012; Kiehl and Shields, 2013). A remaining problem is to understand what combination of radiative forcing and climate sensitivity gave rise to these very elevated temperatures in the first place (Caballero and Huber, 2013). While early Cenozoic CO_2 concentrations are understood to have been higher than modern (Royer, 2014), achieving a good match with reconstructed temperatures using CO_2 alone as the warming agent requires extremely high model CO_2 levels (Lunt et al., 2012), exceeding even the rather loose constraints imposed by the CO_2 proxies.

Non-CO_2 greenhouse gases such as methane and nitrous oxide may have contributed some of the warming (Beerling et al., 2011), but we lack suitable proxies to constrain their concentrations. Another hypothesis is that reduced aerosol loading during the Eocene could play an important role, particularly via its effect on cloud properties (Kump and Pollard, 2008; Kiehl and Shields, 2013). **In a pre-industrial climate aerosol inventories are largely controlled by biological productivity (Andreae, 2007). In a very warm climate, it is possible that temperature limits could be exceeded over large areas of the tropics and subtropics (Huber, 2008) that would sharply limit primary production there, reducing emissions of aerosol precursors to the atmosphere. Further, increased ocean stratification could put further stress on ocean biota, limiting the emission of sulphate precursors (Behrenfeld et al., 2006), while stomatal closure in an elevated CO_2 environment could reduce the emission of organic aerosol precursors from terrestrial plants (Acosta-Navarro et al., 2014). Reduced abundance of aerosols and cloud condensation nuclei is generally thought to lead to larger cloud droplets and reduced cloud albedo (Lohmann and Feichter, 2005)**. A global reduction in aerosol loading would thus lead to lower planetary albedo and a warmer climate. However, we again lack proxies to constrain paleo-aerosol abundances, and cloud-aerosol interactions themselves are still imperfectly understood (Stevens and Feingold, 2009), so this scenario remains highly speculative: **given the current level of understanding, a substantial decrease in aerosol loading and cloud albedo during the Eocene can be neither confirmed nor ruled out with any degree of confidence.** Nonetheless, the problem of disentangling the mix of radiative forcing agents that gave rise to Eocene warmth remains of crucial importance given its implications for climate sensitivity and thus predictions of future climate change (Caballero and Huber, 2013).

Here, we explore the potential for constraining the radiative forcing mix responsible for Eocene warmth *indirectly*—that is, without relying on direct proxies for aerosols or non-CO_2 greenhouse gases. Different combinations of forcing agents supporting the same global-mean surface temperature may leave different signatures in other climatological fields that are potentially detectable in the geological record. We focus specifically on the distinction between warming by greenhouse gases—which affect the longwave radiation—and warming by reduced cloud albedo, which affects solar radiation. We do this by comparing simulations of the Eocene climate warmed with respect to the present solely by increased CO_2**—which we refer to as the greenhouse gas (GHG) scenario—**with simulations using modern pre-industrial CO_2 warmed solely by reduced cloud albedo, but with indistinguishable global-mean surface temperature. As in previous work (Kump and Pollard, 2008; Kiehl and Shields, 2013) we reduce cloud albedo by globally increasing the prescribed size of cloud droplets; we refer to these the "low CO_2–thin clouds" (LCTC) scenario (because the clouds are optically thinner in the shortwave spectrum). We pay particular attention to **differences in surface temperature patterns and to** the hydrological cycle, which is known to respond differently to warming by longwave and shortwave forcing (O'Gorman et al., 2012). A similar discussion arises in the context of geoengineering proposals to artificially increase Earth's planetary albedo in order to offset some of the warming due to anthropogenic CO_2 emissions; it is well known that the resulting climate has a significantly different hydrological cycle compared with a climate subject to the same net radiative forcing but due to a more modest increase in CO_2 (Mcnutt et al., 2015).

Differences in surface temperature patterns and in hydrological regime could potentially be detectable in the terrestrial record, particularly in vegetation. **However, it is not our goal here to provide an exhaustive comparison between our simulations and the extant terrestrial proxy record. Given the broad-brush approach we take, employing a globally-**

uniform increase in cloud droplet radius, it is unlikely that such a detailed comparison would be very meaningful in any case. Instead, we focus on quantifying the differences between the two climates and understanding the climate dynamical processes that lead to these differences, with the aim of assessing whether these differences are large and robust enough to warrant further, more detailed work in this direction.

Our modelling approach is further described in Section 2. Section 3 presents an overview of the climatology in the **GHG** simulation and its changes in the LCTC case. Section 4 discusses the global-mean change in precipitation and its relation to energetic constraints. **Regional climate differences between the two simulations and their relation to circulation changes are discussed in Section 5**. Finally, Section 6 summarizes our conclusions.

2 Methods

2.1 Model and simulations

We employ the Community Atmospheric Model 3.1 (CAM3) developed by the National Center for Atmospheric **Research** (NCAR) (Collins et al., 2006b) at T42 resolution coupled to **the Community Land Model 2 (CLM2) and to a** slab ocean **with uniform 50 m depth**. Ocean heat transport **and seasonal heat storage are** approximated through a prescribed seasonally-varying energy convergence field ("q-flux") derived from a fully-coupled Eocene simulation run to equilibrium for a corresponding climate (Huber and Caballero, 2011). The model is configured with Eocene geography and land surface cover as described in Sewall et al. (2000). Simulation climatologies are computed from 30 years of monthly output obtained after the model has reached equilibrium.

We focus on two end-member simulations of the Eocene: a **GHG** run warmed only by increasing CO_2 and an extreme LCTC run warmed only by decreasing the planetary albedo. In the **GHG** simulation CO_2 is set to 4480 ppm and the **effective cloud droplet radius** takes its default value (8 μm over land and 14 μm over ocean). Various aspects of this simulation have been previously described in previous work (Caballero and Huber, 2010; Huber and Caballero, 2011; Caballero and Huber, 2013). In the LCTC simulation, CO_2 takes its pre-industrial value of 280 ppm while **effective cloud droplet radius** is increased by multiplying the default values by a uniform factor of 2.5, yielding 20 μm over land and 35 μm over ocean Note that this retains the difference between land and ocean values, differently from Kiehl and Shields (2013) who used a single **effective cloud droplet radius** globally. There is little knowledge about the actual aerosol concentration during the Eocene, but present-day observations in remote regions indicate a land-sea difference in droplet size can be expected even in the absence of anthropogenic emissions (Bréon and Colzy, 2000).

These are very large and likely unrealistic droplet sizes, chosen simply because they lead to the same global-mean surface temperature as in the **GHG** run. **In addition, cloud microphysics aside from the effective cloud droplet radius is unchanged, which unrealistically neglects cloud lifetime effects and imposes a further limitation in the interpretation of the results.** Our intention is to compare two end-member states which maximise the difference between the two warming agents. Intermediate combinations of CO_2 and cloud albedo (e.g. Kiehl and Shields, 2013) will presumably have intermediate climate impacts; to test this hypothesis, we also conducted a third simulation where CO_2 is set to 1120 ppm and droplet radii

are scaled by a factor of 1.6, and confirmed that the resulting climate differs from the **GHG** in a qualitatively similar way as described below for the extreme LCTC case, but with smaller overall amplitudes. In the interest of conciseness we focus here only on the end-member cases.

Comparison of the annual-mean surface temperature and precipitation fields in the GHG case (which are presented in the following section) with the corresponding fully-coupled Eocene simulation of Huber and Caballero (2011) show good agreement, with zonal-mean temperature and precipitation differences on the order of $\sim$2 K and $\sim$1 mm day^{-1} respectively. As discussed in Huber and Caballero (2011), the coupled model reproduces the available proxy temperature reconstructions reasonably well, with no appreciable bias in either the global-mean temperature or the mean equator-pole temperature difference. As shown in Carmichael et al. (2016) (where this simulation is referred to as CCSM_H-16x), the precipitation field is also in broad agreement with a global compilation of precipitation proxies, albeit with some mismatches particularly in the Southern Hemisphere high latitudes. This provides confidence that the GHG simulation is a reasonable approximation to the Eocene climate at least in the annual mean. However, seasonal biases are larger, with a reduction of the annual temperature range in mid- to high latitudes of around 5 K in the GHG simulation compared to the full coupled model. This should be born in mind when interpreting the climatologies below. These seasonal biases could possibly be corrected by suitably adjusting the q-flux and/or slab depth. Nonetheless, since our main focus in this paper is on the differences between two simulations using the same slab-ocean configuration, we believe our results should be at least qualitatively robust to the details of the q-flux specification.

3 Climatologies

This section describes the main climatological features of the two simulations, to be further analysed and interpreted in subsequent sections.

Zonal- and annual-mean profiles of surface temperature and precipitation for the two simulations are presented in Figure 1. Despite their very different radiative forcing agents, the two simulations have almost identical zonal-mean temperatures, **differing at most by around 0.9 K**. In the global mean, the LCTC simulation is cooler by 0.3 K than the **GHG** simulation. Precipitation, on the other hand, is significantly larger in the LCTC case, especially in the tropics and in the subtropical flanks of the major midlatitude precipitation zones.

As shown in Figure 2b, however, regional differences in surface temperature are large. Land areas are cooler in the LCTC run by up to 5 K, particularly in subtropical regions with little cloud cover (Figure 2e), **the annual-mean climatology in the LCTC case is shown in Figure S1 in the supplementary material**. Offsetting warming develops over the oceans, notably in twin horseshoe-shaped regions of the Pacific in both hemispheres. These temperature responses are accompanied by large changes in the low-level circulation (Figure 2b). The LCTC case exhibits a cyclonic anomaly over the northern Pacific, with a similar but weaker response over the southern Pacific. The cyclonic anomaly acts to weaken the prevailing subtropical **anticyclones** seen in the **GHG** case (Figure 2a). This is reminiscent of the weakening of the subtropical anticyclones seen in the transition from summer to winter in the modern day, which is also accompanied by a cooling of the continents relative to the oceans.

While global-mean temperature is **very similar** in the two simulations, global-mean precipitation is **3.8 mm day^{-1} in the GHG simulation and 0.43 mm day^{-1}** or about 11% higher in the LCTC case. This must be considered a substantial increase: Carmichael et al. (2016, their Figure 2c) show a robust linear scaling of precipitation with temperature of around 0.06 mm day^{-1} K^{-1}, implying that a precipitation increase of this magnitude would require a CO_2-driven warming in excess of 7 K (comparable to that across the Paleocene-Eocene Thermal Maximum (PETM) hyperthermal event, see Pagani et al., 2014). **For comparison, a present-day simulation using CAM3 (Collins et al., 2006a) has global-mean temperature around 15 K cooler and precipitation around 0.9 mm day^{-1} lower than the GHG simulation, in agreement with the scaling above.**

As shown in Figure 2d the spatial distribution of the precipitation change is highly non-uniform, with regional increases well in excess of 100%. The greatest precipitation increase is concentrated in the central and eastern equatorial Pacific, partly offset by a large decrease in the western Pacific Warm Pool region. Precipitation also increases across large swaths of the subtropical to midlatitude Pacific and Atlantic Oceans and adjacent land areas.

Cloud cover in the **GHG** simulation (Figure 2e) shows broad-scale structures similar to the modern day, with abundant cloud cover over the Pacific Warm Pool and intertropical convergence zones (ITCZ) and over the midlatitude oceanic storm tracks and extensive stratocumulus decks in the eastern subtropical margins of the main ocean basins. Though our LCTC simulation only prescribes changes in cloud droplet size **and CO_2**, the resulting dynamical and thermodynamical changes lead to changes also in cloud **fraction** (Figure 2f). In particular, there is a substantial decrease in cloud fraction in the North Pacific subtropics—in the same region showing a large sea-surface temperature (SST) warming (Figure 2b)—and increased cloud cover over southwestern North America, associated with increased precipitation there (Figure 2d).

Figures 2g,h examine the atmospheric jets and storm tracks in the two simulations. As in the modern climate, zonal winds in the Northern Hemisphere of the **GHG** simulation are concentrated into separate jet streams spanning the Pacific and Atlantic basins; differently from modern, the Pacific jet exhibits a marked meridional tilt. **The Pacific jet's modern structure is well represented in modern-day simulations using CAM3 (Hurrell et al., 2006), so the jet's meridional tilt in our GHG simulation appears to be an intrinsic feature of this climate state, potentially related to its high CO_2 (Grise and Polvani, 2013) and to the structure of Asian orography, which lacks the modern Tibetan Plateau and instead presents a more continuous north-south obstacle with modest elevation (Brayshaw et al., 2009; Löfverström et al., 2016).** The jets are associated with regions of enhanced eddy variability—storm tracks—which are grossly identified here by the sub-monthly eddy kinetic energy EKE $= (u'^2 + v'^2)/2$, where u and v are zonal and meridional components of the wind and primes denote sub-monthly deviations from monthly climatology. Lower-tropospheric jets and storm tracks are intimately connected via wave-mean flow interaction (Shaw et al., 2016). In the **GHG** run, the North Pacific storm track is further northward than observed in the modern climate (Shaw et al., 2016), consistent with the strong meridional tilt of the Pacific jet. In the LCTC case, however, the North Pacific jet and storm track show a marked equatorward shift, with enhanced winds and EKE in the subtropical basin and reductions further north. In the Southern Hemisphere the jet and storm tracks are more zonally continuous, but a similar equatorward shift can be observed in the LCTC case. Along the equator, the LCTC case shows a low-level westerly wind anomaly in the western Pacific, consistent with a weakening of the Walker Cell and an eastward shift of precipitation

towards the central Pacific as noted above. There is also a marked reduction in EKE in the western equatorial Pacific, in the same region where precipitation decreases. Much of the sub-seasonal variability in the tropics is due to the Madden-Julian Oscillation (MJO). As discussed elsewhere (Caballero and Huber, 2010; Arnold et al., 2014; Carlson and Caballero, 2016), warm climates show a strongly enhanced MJO in a range of climate models including the one used here. It is possible that the MJO is more muted in the LCTC simulation, perhaps because of changes in the Walker Cell, but we do not investigate this issue further here.

Figure 3 compares the two simulations' annual and diurnal surface temperature ranges, which play an important role in determining both floral and faunal species ranges (Pearson and Dawson, 2003). Monthly-mean temperatures during the warmest month in the GHG simulation are above 320 K over large parts of the subtropical continents (Figure 3a), potentially exceeding the survivability limits of vegetation there (Huber, 2008). These regions are cooler in the LCTC case (Figure 3b) due to generally low cloud cover there—which limits the warming effect of thinner clouds—combined with the lower CO_2. This LCTC cooling, though modest (generally around 3-5 K) could facilitate the survival of plants over the summer. Palynological evidence from northwestern South America (Jaramillo et al., 2006) indicates high floral biodiversity there, suggesting little environmental stress; however, this evidence comes from a near-equatorial region where both simulations show more moderate warm-month temperatures in addition to high precipitation. Floral reconstructions directly relevant to the extremely warm subtropical regions appear to be lacking at present. At higher latitudes, summer temperatures are somewhat warmer in the LCTC than the GHG case, presumably because high cloud cover there allows the warming effect of thinner clouds to dominate over the reduction in CO_2.

Cold-month temperatures are above freezing everywhere in the GHG simulation except for parts of eastern Asia and North America (identified by white contours in Figure 3c). In the LCTC simulation, cold-month temperatures are generally cooler, consistent with a weaker warming effect by thin clouds during winter when insolation is low. This leads to a moderate expansion of the regions experiencing sub-freezing winter temperatures, though importantly both the Arctic Ocean and Antarctica remain above freezing. There is substantial fossil evidence for subtropical, frost-intolerant flora and fauna surviving in western continental interiors and along the margins of the Arctic Ocean during the early Eocene (Markwick, 1998; Greenwood and Wing, 1995), and both GHG and LCTC simulations are largely compatible with such evidence.

Lastly, we turn to the diurnal surface temperature range, estimated as the difference in monthly-mean maximum and minimum temperatures at each grid point (these quantities are not available in the model output over oceans, so only land values are shown in Figures 3e,f). The annual-mean diurnal temperature range in the GHG simulation (Figure 3e) is large over parts of the subtropical continents, particularly in western Asia and North America where it locally exceeds 16 K, consistent with low cloudiness in those regions. In the LCTC case, the diurnal temperature range is modestly larger over most continental regions; this enhancement in the LCTC case can be ascribed to greater daytime heating due to reduced cloud albedos and greater nighttime cooling due to reduced CO_2. The enhancement is markedly stronger over subtropical and midlatitude Asia, where it is up to 50% greater than in the GHG case, which we ascribe to the substantial decrease in cloud cover in that region (Figure 2f). Conversely, subtropical North America experiences

a diurnal temperature range around 20% smaller than in the GHG case, consistent with increased cloud cover there which overcompensates for the reduced cloud albedo.

4 Global-mean precipitation and energetic constraints

As noted above, global-mean precipitation in the LCTC case is around 11% higher than in the **GHG**. A precipitation increase in response to a simultaneous drop in CO_2 and planetary albedo is consistent with simulations of geoengineering scenarios, where increased CO_2 and planetary albedo lead to lower precipitation (Bala et al., 2008). In this section we account for the global-mean precipitation change in our simulations from the perspective of energy budget constraints (O'Gorman et al., 2012).

The global-mean atmospheric energy budget can be written, assuming steady state, as

$$SW_{TOA} - SW_{srf} + LW_{TOA} - LW_{srf} - LH - SH = 0, \tag{1}$$

where SW and LW refer to shortwave and longwave radiation with subscripts TOA and srf indicating top-of-atmosphere and surface fluxes respectively, while LH and SH are surface latent and sensible heat fluxes respectively. All fluxes are taken to be positive downwards. Given the atmospheric steady state assumption, $LH = -L_v P$, where P is global-mean precipitation and L_v the latent heat capacity. If the planet as a whole is also in steady state, then $SW_{TOA} + LW_{TOA} = 0$ and (1) reduces to the surface energy budget

$$SW_{srf} + LW_{srf} + LH + SH = 0. \tag{2}$$

For climates in planetary energy balance, like those studied here, the atmospheric and surface energy budgets are thus equivalent, and provide alternative and complementary perspectives on the mechanisms controlling changes in precipitation (Allen and Ingram, 2002; Pierrehumbert, 2002). We examine both perspectives here.

The terms in (1) for the **GHG** case are shown in Figure 4a. **The LH is the largest component**, but shortwave absorption ($SW_{TOA} - SW_{srf}$) also makes a large contribution as can be expected in this very warm and thus moist climate. Sensible heating makes a much smaller contribution. The heating is entirely balanced by net longwave cooling ($LW_{TOA} - LW_{srf}$). Changes when going to the LCTC case are shown in Figure 4b. Net longwave cooling increases by about 17 W m^{-2} in the LCTC run. This increased cooling is a combination of clear-sky and cloud effects. In clear skies, lowering CO_2 while keeping temperature and humidity fixed yields stronger outgoing longwave radiation at the TOA (which increases atmospheric cooling) and weaker downward radiation at the surface (which decreases cooling). The former effect dominates the latter, however (Pendergrass and Hartmann, 2014), so the net result is increased cooling. The contribution of cloud effects can be estimated using the cloud radiative effect (CRE, difference between all-sky and clear-sky radiation). Net atmospheric longwave CRE—the difference between TOA and surface CRE—is about 13 W m^{-2} in the **GHG** case, implying clouds have a net heating effect in the longwave. This heating drops to 7 W m^{-2} in the LCTC case, which means that **cloud changes**—including the general reduction in cloud cover seen in Figure 2f **as well as changes in cloud LW opacity due to increased effective drop radius—make a substantial contribution of** around 6 W m^{-2} to the 17 W m^{-2} total increase in atmospheric cooling. Finally,

Figure 4b also shows that increased longwave cooling is balanced mostly by latent heating, with sensible heating and shortwave absorption playing minor roles. In summary, the atmospheric energy budget perspective indicates that precipitation increases in the LCTC run to compensate for increased longwave cooling due mostly to the clear-sky effect of reduced CO_2, with **a substantial** contribution also from changes in cloud **fraction and emissivity**.

From the surface budget perspective (2), Figure 4b (noting the reversed sign convention) shows that increased shortwave heating of the surface in the LCTC case—due to the lower cloud albedo—is mainly compensated through increased latent heat flux and also increased longwave surface cooling (due to reduced downwelling radiation, as noted above). From the surface perspective, then, precipitation increases in the LCTC case mostly to balance increased surface solar heating. This points to a rather different physical picture than the atmospheric perspective, in which shortwave fluxes play a negligible role. Given the equivalence of (1) and (2), the two physical pictures must of course be consistent. A plausible hypothesis for how consistency is achieved runs as follows: atmospheric destabilization by radiative cooling due to reduced CO_2 accelerates convection, increasing rainfall and also mixing drier air down into the boundary layer; this drying increases evaporative demand at the surface, and the extra energy required to maintain surface temperature against evaporative cooling is supplied by increased solar absorption due to reduced cloud albedo. Fully reconciling the two perspectives in a causal, mechanistic way would require considerably more work going beyond the scope of this paper. However, some evidence supporting this hypothesis is shown in the following section.

5 Atmospheric circulation and regional climate response

While the energetic constraints discussed above help explain the global increase in precipitation in the LCTC case, they place no constraints on its spatial distribution, which is highly heterogeneous (Figure 2d). These regional changes in precipitation are accompanied by pronounced changes in the surface temperature pattern (Figure 2b) and the atmospheric general circulation (Figure 2h). In this section we explore how these various changes are interrelated. To do this, it is useful to think of the transition from the **GHG** to the LCTC climate as if it occurred in 3 stages: first CO_2 is reduced instantaneously, producing a fast adjustment in the atmosphere and land before SST has time to change (Sherwood et al., 2015); then cloud albedo is instantaneously reduced, producing a further fast adjustment; and finally the SST slowly adjusts to its final equilibrium pattern. Circulation changes linked to the fast adjustments will condition the evolution of the SST pattern, which in turn will affect the circulation.

We make this conceptual picture quantitative by running 3 fixed-SST experiments. Two employ prescribed (seasonally-varying) SST from the **GHG** run; one uses **GHG** values of cloud drop radius while CO_2 is reduced to 280 ppm while the other uses **GHG** CO_2 and cloud drop radius increased by a factor of 2.5. The third run uses **GHG** values of CO_2 and cloud drop radius but prescribes the SST from the LCTC case. Comparing these fixed-SST simulations with the **GHG** run allows us to separately quantify the effect of changing CO_2, cloud albedo and SST pattern.

Figure 5 shows the surface temperature and low-level circulation responses in the three simulations. The sum of all changes (Figure 5d) gives a reasonable match to the full response in the LCTC run (Figure 2b), though with somewhat higher amplitude,

suggesting that this linear decomposition is an adequate approximation. The direct response to reduced CO_2 (Figure 5a) involves strong cooling of the extratropical continents and a basin-scale cyclonic anomaly over both the North and South Pacific, with westerly anomalies spanning the tropics and lower midlatitudes and easterly anomalies further north. This is accompanied by an equatorward migration of the upper level jets in both hemispheres, consistently with previous work (Grise and Polvani, 2013). Cooling of midlatitude land relative to the ocean accompanied by cyclonic anomalies over the ocean is reminiscent of the negative phase of the "cold ocean–warm land" pattern (Wallace et al., 1996). It is also consistent with the work of Molteni et al. (2011), who show cyclonic anomalies over the North Pacific in simulations with permanently increased land-ocean temperature contrast and explore alternative dynamical scenarios to account for them.

The direct response to cloud albedo reduction (Figure 5b) is a warming of the continents, particularly at high latitudes. This warming is highly seasonal, peaking in the summer, unlike the CO_2 response which is more even through the year. Somewhat surprisingly, the circulation response to continental warming is weak and not obviously anticyclonic except in the South Pacific. The reasons for this weak response are unclear; it is perhaps due to the seasonal and high-latitude nature of the warming, but we do not explore the issue further here.

Finally, the response to changing SST pattern (Figure 5c) features a strong cyclonic anomaly over the North Pacific—where the SST anomaly is strongest—and a weaker cyclonic anomaly over the South Pacific. In the extratropics of both hemispheres, the circulation responses align with those induced by CO_2 alone, and similarly yield an equatorward shift of the lower-tropospheric jets. There is also a strong response in the tropics, in particular an **westerly** anomaly in the tropical west Pacific indicating a weakened Walker cell consistent with the substantial warm anomalies in the central Pacific.

Precipitation changes from the **GHG** for the 3 runs are presented in Figure 6. The sum of all changes (Figure 6d) again captures the change seen in the full LCTC case (Figure 2d) reasonably well. Global-mean precipitation increases by 0.37 mm day^{-1} in response to CO_2 alone, by 0.05 mm day^{-1} in response to cloud albedo alone and decreases slightly in response to SST pattern. Thus, most of the 0.42 mm day^{-1} increase seen in the LCTC run is due to the direct effect of CO_2. Reduced cloud albedo drives little change in precipitation by itself—instead, as discussed at the end of Section 4, it serves to close the surface energy balance, supplying surface solar heating to offset increased evaporative cooling. While CO_2 drives most of the global-mean precipitation change, its spatial pattern (Figure 6a) shows anomalies concentrated in the eastern Pacific and over the Indo-Pacific warm pool, which is very different from that in the final state (Figure 2d). Changes in SST pattern clearly play a major role in redistributing tropical precipitation into the central Pacific (Figure 6c), consistent with warm SST anomalies there enhancing low-level convergence as is evident in Figure 5c.

Taken together, these results indicate a key role for the SST pattern in mediating the transition from the **GHG** to the LCTC climate state. So what gives rise to the SST anomaly? Some insight into this question is provided by the work of Vimont et al. (2001), who argue that a cyclonic circulation anomaly in the extratropical North Pacific will yield an SST "footprint" which has precisely the horseshoe structure we find here (compare their Figure 1 with Figure 2b). This happens because the anomalous surface winds affect surface energy fluxes. This interpretation is supported by Figure 7, which shows the net surface energy flux change from the **GHG** to the fixed-SST low CO_2 simulation. The pattern of ocean heating and cooling induced by these surface flux anomalies clearly aligns well with the SST anomaly (Figure 5c). Note in particular that the surface energy flux

anomaly will tend to warm the central Pacific relative to the rest of the equatorial zone, driving a shift in precipitation into the central Pacific.

A further important point highlighted by Figure 5c is that the SST anomaly itself produces an extratropical circulation response that superposes constructively on the pre-existing CO_2-induced cyclonic circulation anomaly. Given the generally weak atmospheric response to extratropical SST anomalies (Kushnir et al., 2002), it is most likely that this extratropical circulation response is driven from the tropics, in particular by warm SST anomaly in the central Pacific which—as noted above—promotes large precipitation anomalies there, much like in an El Niño event. Such tropical heating anomalies are known to robustly induce cyclonic circulation anomalies in the extratropical North Pacific (Alexander et al., 2002). Furthermore, it is well known from both observations (Caballero, 2007) and model studies (Tandon et al., 2013) that El Niño events and their associated tropical heating anomalies drive an equatorward shift of the extratropical jets and storm tracks, in agreement with what we find here (Figure 2h).

In summary, the picture that emerges is that the direct effect of reduced CO_2 initially drives a basin-scale cyclonic circulation anomaly in each hemisphere of the Pacific Ocean; this circulation anomaly then drives SST anomalies which reinforce the initial response to CO_2. The direct response to cloud albedo appears to play a minor role in driving regional climate changes. This picture points to an important limitation of our modelling approach, which uses a slab ocean model. With a dynamic ocean, the westerly wind anomalies along the equator (Figure 7) would likely drive a deepening of the ocean thermocline in the eastern equatorial Pacific, shifting the mean climate towards a more El Niño-like state. This response and its global consequences are an important target for future work using a fully-coupled modelling approach.

6 Conclusions

We have studied the differences in circulation and hydrological cycle resulting from two extreme scenarios by which Eocene simulations can attain surface temperatures compatible with proxy reconstructions: one by warming exclusively by increased CO_2 (the **GHG** case), the other by warming exclusively via reduced cloud albedo (the LCTC case). The two simulations have essentially identical zonal-mean surface temperature, but the LCTC case has significantly higher precipitation. Analysis of the global-mean energy budget (Section 4) suggests that the increased precipitation can be viewed as resulting from greater radiative cooling of the atmosphere in the LCTC case due to its lower CO_2. The spatial distribution of the precipitation increase is highly heterogeneous, and is concentrated largely in the central equatorial Pacific and in the lower midlatitudes. The midlatitude continents cool in the LCTC simulation, with compensating warming of the oceans particular in horseshoe-shaped patterns in both hemispheres of the Pacific. There are also major changes to the atmospheric circulation, with basin-scale cyclonic anomalies appearing in both hemispheres of the Pacific associated with equatorward shifts of the storm tracks, and a strong weakening of the Walker Cell in the tropics.

More detailed analysis (Section 5) suggests that these various anomalies are dynamically interrelated. Lower CO_2 in the LCTC case leads to continental cooling, which in turn generates cyclonic circulation anomalies over the Pacific. We propose that these cyclonic anomalies in turn leave a horseshoe shaped "footprint" on SSTs via their effect on surface turbulent fluxes

(Vimont et al., 2001). This footprint reaches into the central tropical Pacific and promotes increased convection there which, much as in a modern El Niño event, affects the extratropical circulation and enhances the pre-existing cyclonic anomalies. **This self-reinforcing mechanism leads to the pronounced regional climate anomalies noted above, which may also affect adjacent land areas.**

Our work is intended as an initial exploration, and much work remains to be done to remove the limitations imposed by our choice of a relatively simplified modelling approach. A key limitation is our use of a slab ocean. As noted in Section 5, the ocean will dynamically respond to the westerly surface stress anomalies along the equator (Vimont et al., 2001), possibly leading to a climate state with a permanently reduced tropical thermocline tilt and a more El Niño-like climate. If this were the case, the ocean dynamical response would in fact further strengthen the tropical anomalies found here, which already resemble an El Niño-like response. Another important caveat is that circulation responses to changes in radiative forcing—and their associated regional climate changes—are sensitive to biases in the unperturbed state (Shepherd, 2014). For example, if the Pacific jet were more zonally oriented in reality than in our **GHG** Eocene simulation (Figure 2g), its response in the LCTC scenario could be quite different. A further limitation of our approach is the specification of a uniformly increased cloud drop radius, leaving other aspects of cloud microphysics untouched. This is highly unrealistic in several ways: there is no particular reason to expect that different cloud types would respond in the same way to reduced aerosol loading; moreover, larger cloud drops are expected to coalesce more readily and thus reduce cloud lifetimes, potentially leading to reductions in cloud cover which would be different for different cloud types. In addition, all the above effects would depend on the precise nature and composition of natural aerosol in the Eocene, which remains essentially unknown. Different hypotheses for aerosol composition and cloud microphysics could lead to very different spatial structures of the resulting radiative forcing, with potentially large impacts on the circulation and regional climates.

Despite these important caveats, we conclude that differences in the radiative forcing agent driving Eocene warmth could at least in principle lead to large differences in regional climates leaving potentially detectable traces in the geological record. We have explored here two end-member scenarios, one with very high CO_2 (higher than suggested by current CO_2 proxy reconstructions) and another with pre-industrial CO_2 (which is almost certainly lower than in the Eocene). A more realistic scenario would involve some intermediate mix of warming by CO_2 and by cloud effects (Kiehl and Shields, 2013), which would be expected to yield smaller climate differences than those found here. However, given the large uncertainties discussed above, it remains possible that even an intermediate mix of warming agents could lead to responses as large or larger than those in our study. Future work with a range of models including more complete representations of ocean dynamics and cloud-aerosol interactions is required to settle this question.

Acknowledgements. We thank Qiang Fu, Jack Scheff and Johan Nilsson for useful discussion and comments. The Swedish National Infrastructure for Computing (SNIC) at the National Supercomputing Centre (NSC), Linköping University, provided the high performance computing resources to perform the simulations.

References

Acosta-Navarro, J. C., Smolander, S., Struthers, H., Zorita, E., Ekman, A. M., Kaplan, J., Guenther, A., Arneth, A., and Riipinen, I.: Global emissions of terpenoid VOCs from terrestrial vegetation in the last millennium, J. Geophys. Res. Oceans, 119, 6867–6885, 2014.

Alexander, M. A., Bladé, I., Newman, M., Lanzante, J. R., Lau, N.-C., and Scott, J. D.: The atmospheric bridge: The influence of ENSO teleconnections on air–sea interaction over the global oceans, J. Climate, 15, 2205–2231, 2002.

Allen, M. R. and Ingram, W. J.: Constraints on future changes in climate and the hydrologic cycle, Nature, 419, 224–232, 2002.

Andreae, M. O.: ATMOSPHERE: Aerosols Before Pollution, Science, 315, 50–51, 2007.

Arnold, N. P., Branson, M., Burt, M. A., Abbot, D. S., Kuang, Z., Randall, D. A., and Tziperman, E.: Effects of explicit atmospheric convection at high CO_2, Proc. Natl. Acad. Sci. USA, 111, 10 943–10 948, 2014.

Bala, G., Duffy, P., and Taylor, K.: Impact of geoengineering schemes on the global hydrological cycle, Proc. Natl. Acad. Sci. USA, 105, 7664–7669, 2008.

Beerling, D. J., Fox, A., Stevenson, D. S., and Valdes, P. J.: Enhanced chemistry-climate feedbacks in past greenhouse worlds, Proc. Natl. Acad. Sci. USA, 108, 9770–9775, 2011.

Behrenfeld, M. J., O'Malley, R. T., Siegel, D. A., McClain, C. R., Sarmiento, J. L., Feldman, G. C., Milligan, A. J., Falkowski, P. G., Letelier, R. M., and Boss, E. S.: Climate-driven trends in contemporary ocean productivity, Nature, 444, 752–755, 2006.

Brayshaw, D. J., Hoskins, B., and Blackburn, M.: The basic ingredients of the North Atlantic storm track. Part I: Land–sea contrast and orography, J. Atmos. Sci., 66, 2539–2558, 2009.

Bréon, F.-M. and Colzy, S.: Global distribution of cloud droplet effective radius from POLDER polarization measurements, Geophys. Res. Lett., 27, 4065–4068, 2000.

Caballero, R.: Role of eddies in the interannual variability of Hadley cell strength, Geophys. Res. Lett., 34, L22 705, 2007.

Caballero, R. and Huber, M.: Spontaneous transition to superrotation in warm climates simulated by CAM3, Geophys. Res. Lett, 37, L11 701, 2010.

Caballero, R. and Huber, M.: State-dependent climate sensitivity in past warm climates and its implications for future climate projections, Proc. Natl. Acad. Sci. USA, 110, 14 162–14 167, doi:10.1073/pnas.1303365110, http://dx.doi.org/10.1073/pnas.1303365110, 2013.

Carlson, H. and Caballero, R.: Enhanced MJO and transition to superrotation in warm climates, J. Adv. Model. Earth Syst., 8, 304–318, 2016.

Carmichael, M. J., Lunt, D. J., Huber, M., Heinemann, M., Kiehl, J., LeGrande, A., Loptson, C. A., Roberts, C. D., Sagoo, N., Shields, C., Valdes, P. J., Winguth, A., Winguth, C., and Pancost, R. D.: A model-model and data-model comparison for the early Eocene hydrological cycle, Climate of the Past, 12, 455–481, 2016.

Collins, W., Bitz, C., Blackmon, M., Bonan, G., Bretherton, C., Carton, J., Chang, P., Doney, S., Hack, J., Henderson, T., et al.: The Community Climate System Model Version 3 (CCSM3), jclim, 19, 2122–2143, 2006a.

Collins, W. D., Rasch, P. J., Boville, B. A., Hack, J. J., McCaa, J. R., Williamson, D. L., Briegleb, B. P., Bitz, C. M., Lin, S.-J., and Zhang, M.: The Formulation and Atmospheric Simulation of the Community Atmosphere Model Version 3 (CAM3), J. Climate, 19, 2144–2161, doi:10.1175/JCLI3760.1, http://dx.doi.org/10.1175/JCLI3760.1, 2006b.

Greenwood, D. R. and Wing, S. L.: Eocene continental climates and latitudinal temperature gradients, Geology, 23, 1044–1048, 1995.

Grise, K. M. and Polvani, L. M.: Is climate sensitivity related to dynamical sensitivity? A Southern Hemisphere perspective, Geophys. Res. Lett., pp. n/a–n/a, doi:10.1002/2013GL058466, http://dx.doi.org/10.1002/2013GL058466, 2013.

Huber, M.: CLIMATE CHANGE: A Hotter Greenhouse?, Science, 321, 353–354, doi:10.1126/science.1161170, http://dx.doi.org/10.1126/science.1161170, 2008.

Huber, M. and Caballero, R.: The early Eocene equable climate problem revisited, Climate of the Past, 7, 603–633, doi:10.5194/cp-7-603-2011, http://dx.doi.org/10.5194/cp-7-603-2011, 2011.

Hurrell, J. W., Hack, J. J., Phillips, A. S., Caron, J., and Yin, J.: The dynamical simulation of the Community Atmosphere Model version 3 (CAM3), J. Climate, 19, 2162–2183, 2006.

Jaramillo, C., Rueda, M. J., and Mora, G.: Cenozoic plant diversity in the Neotropics, Science, 311, 1893–1896, 2006.

Kiehl, J. T. and Shields, C. A.: Sensitivity of the Palaeocene-Eocene Thermal Maximum climate to cloud properties, Philosophical Transactions of the Royal Society A: Mathematical, Physical and Engineering Sciences, 371, 20130 093, doi:10.1098/rsta.2013.0093, http://dx.doi.org/10.1098/rsta.2013.0093, 2013.

Kump, L. R. and Pollard, D.: Amplification of Cretaceous Warmth by Biological Cloud Feedbacks, Science, 320, 195, doi:10.1126/science.1153883, http://dx.doi.org/10.1126/science.1153883, 2008.

Kushnir, Y., Robinson, W., Bladé, I., Hall, N., Peng, S., and Sutton, R.: Atmospheric GCM response to extratropical SST anomalies: Synthesis and evaluation, J. Climate, 15, 2233–2256, 2002.

Löfverström, M., Caballero, R., Nilsson, J., and Messori, G.: Stationary wave reflection as a mechanism for zonalising the Atlantic winter jet at the LGM, J. Atmos. Sci., 73, 3329–3342, 2016.

Lohmann, U. and Feichter, J.: Global indirect aerosol effects: a review, Atmos. Chem. Phys., 5, 715–737, 2005.

Lunt, D. J., Dunkley Jones, T., Heinemann, M., Huber, M., LeGrande, A., Winguth, A., Loptson, C., Marotzke, J., Roberts, C., Tindall, J., et al.: A model–data comparison for a multi-model ensemble of early Eocene atmosphere–ocean simulations: EoMIP, Clim. Past, 8, 1717–1736, 2012.

Markwick, P. J.: Fossil crocodilians as indicators of Late Cretaceous and Cenozoic climates: implications for using palaeontological data in reconstructing palaeoclimate, Palaeogeog. Palaeoclim. Palaeoecol., 137, 205–271, 1998.

Mcnutt, M. K., Abdalati, W., Caldeira, K., Doney, S. C., Falkowski, P. G., Fetter, S., Fleming, J. R., Hamburg, S. P., Morgan, M. G., Penner, J. E., et al.: Climate Intervention: Reflecting Sunlight to Cool Earth, National Academy of Sciences: Washington, DC, USA, 2015.

Molteni, F., King, M. P., Kucharski, F., and Straus, D. M.: Planetary-scale variability in the northern winter and the impact of land–sea thermal contrast, Clim. Dyn., 37, 151–170, 2011.

O'Gorman, P. A., Allan, R. P., Byrne, M. P., and Previdi, M.: Energetic constraints on precipitation under climate change, Surv. Geophys., 33, 585–608, 2012.

Pagani, M., Huber, M., and Sageman, B.: Greenhouse climates, in: Treatise on Geochemistry, edited by Holland, H. and Turekian, K., pp. 281–304, Elsevier, Oxford, second edn., 2014.

Pearson, R. G. and Dawson, T. P.: Predicting the impacts of climate change on the distribution of species: are bioclimate envelope models useful?, Glob. Ecol. Biogeog., 12, 361–371, 2003.

Pendergrass, A. G. and Hartmann, D. L.: The Atmospheric Energy Constraint on Global-Mean Precipitation Change, Journal of Climate, 27, 757–768, 2014.

Pierrehumbert, R. T.: The hydrologic cycle in deep-time climate problems, Nature, 419, 191–198, doi:10.1038/nature01088, http://dx.doi.org/10.1038/nature01088, 2002.

Royer, D.: Atmospheric CO_2 and O_2 during the Phanerozoic: Tools, patterns, and impacts, in: Treatise on Geochemistry, edited by Holland, H. and Turekian, K., pp. 251–267, Elsevier, second edition edn., 2014.

Sewall, J. O., Sloan, L. C., Huber, M., and Wing, S.: Climate sensitivity to changes in land surface characteristics, Global Planet. Change, 26, 445–465, 2000.

Shaw, T. A., Baldwin, M., Barnes, E. A., Caballero, R., Garfinkel, C. I., Hwang, Y. T., Li, C., O'Gorman, P. A., Riviere, G., Simpson, I. R., and Voigt, A.: Storm track processes and the opposing influences of climate change, Nat. Geosci., p. doi:10.1038/ngeo2783, 2016.

Shepherd, T. G.: Atmospheric circulation as a source of uncertainty in climate change projections, Nat. Geosci., 7, 703–708, 2014.

Sherwood, S. C., Bony, S., Boucher, O., Bretherton, C., Forster, P. M., Gregory, J. M., and Stevens, B.: Adjustments in the forcing-feedback framework for understanding climate change, Bull. Am. Meteorol. Soc., 96, 217–228, 2015.

Stevens, B. and Feingold, G.: Untangling aerosol effects on clouds and precipitation in a buffered system, Nature, 461, 607–613, 2009.

Tandon, N. F., Gerber, E. P., Sobel, A. H., and Polvani, L. M.: Understanding Hadley cell expansion versus contraction: Insights from simplified models and implications for recent observations, J. Clim., 26, 4304–4321, 2013.

Vimont, D., Battisti, D., and Hirst, A.: Footprinting: A seasonal connection between the tropics and mid-latitudes, Geophys. Res. Lett., 28, 3923–3926, 2001.

Wallace, J. M., Zhang, Y., and Bajuk, L.: Interpretation of interdecadal trends in Northern Hemisphere surface air temperature, J. Climate, 9, 249–259, 1996.

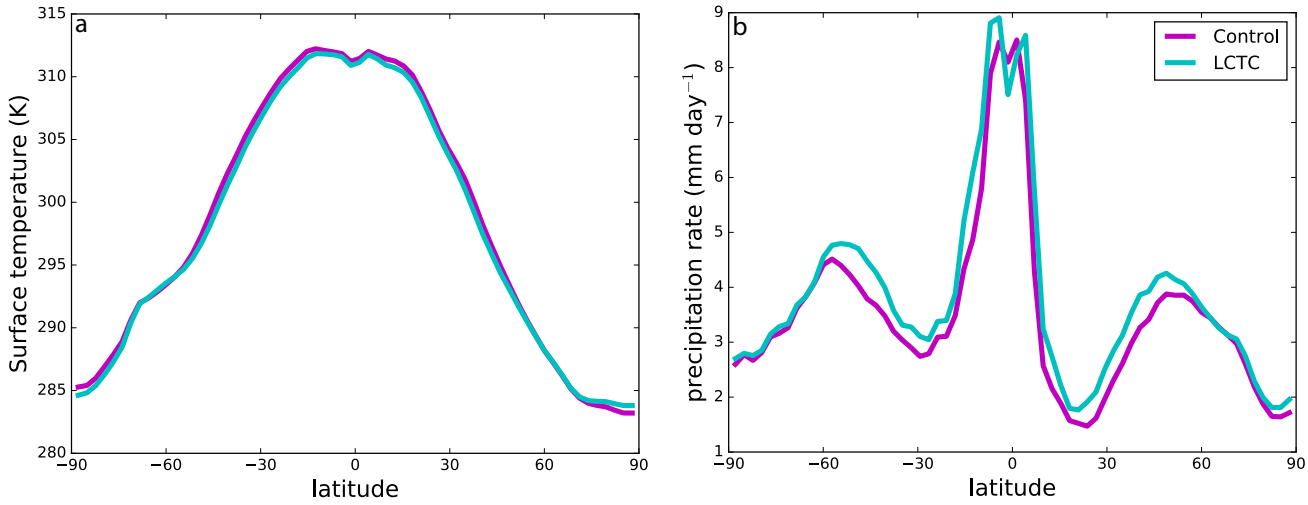

Figure 1. Annual- and zonal-mean surface temperature (a) and precipitation (b) in the **GHG** case (magenta) and LCTC case (cyan).

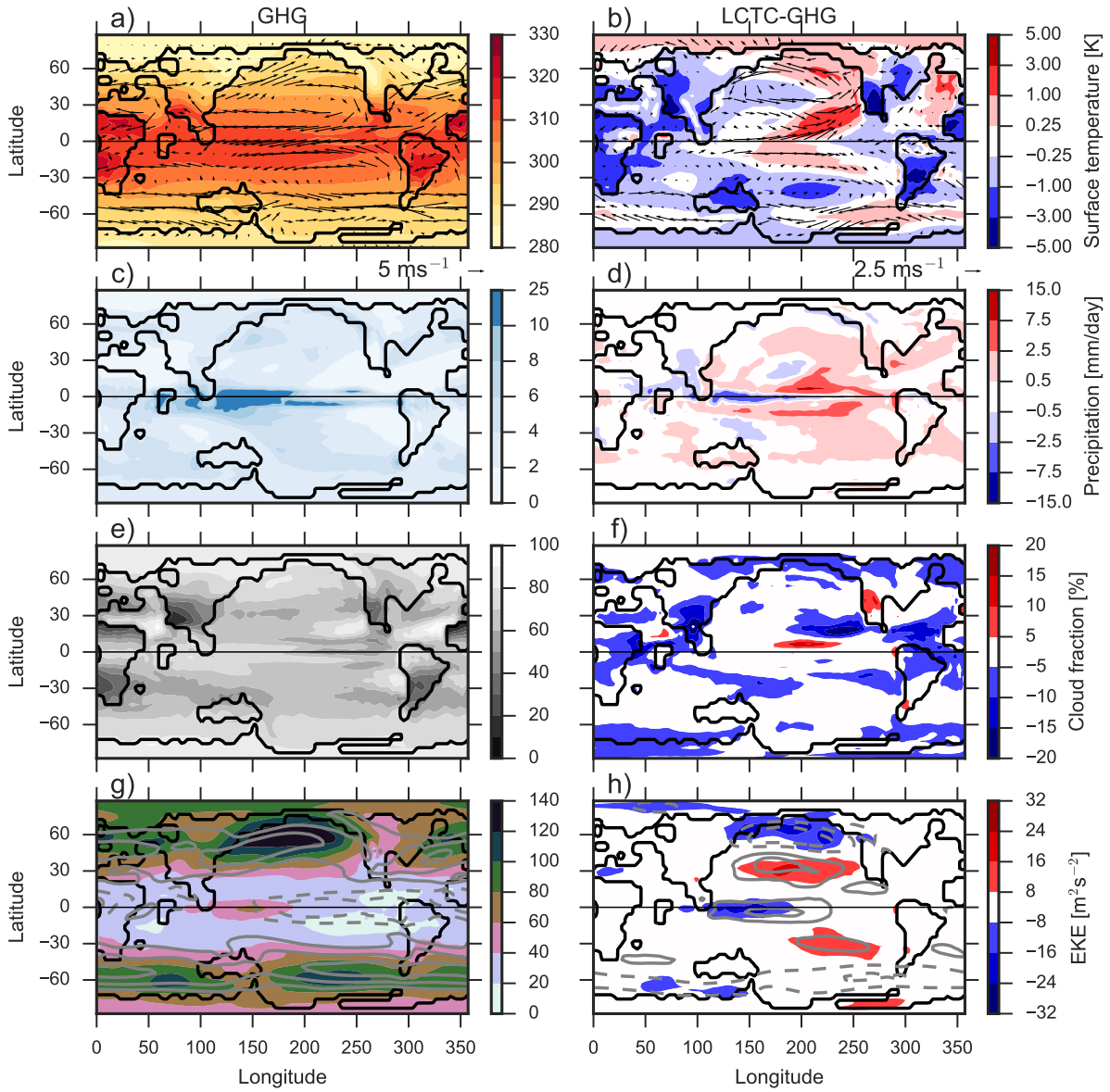

Figure 2. Annual-mean climatology in the **GHG** run (left column) and its change in the LCTC case (right column) of (a,b) surface temperature (shading) and 900 hPa wind (arrows); (c,d) precipitation; (e,f) cloud fraction and (g,h) eddy kinetic energy (shading) and zonal wind at 700 hPa (contours, c.i. 4 ms^{-1} in (g) and 2 ms^{-1} in (h)).

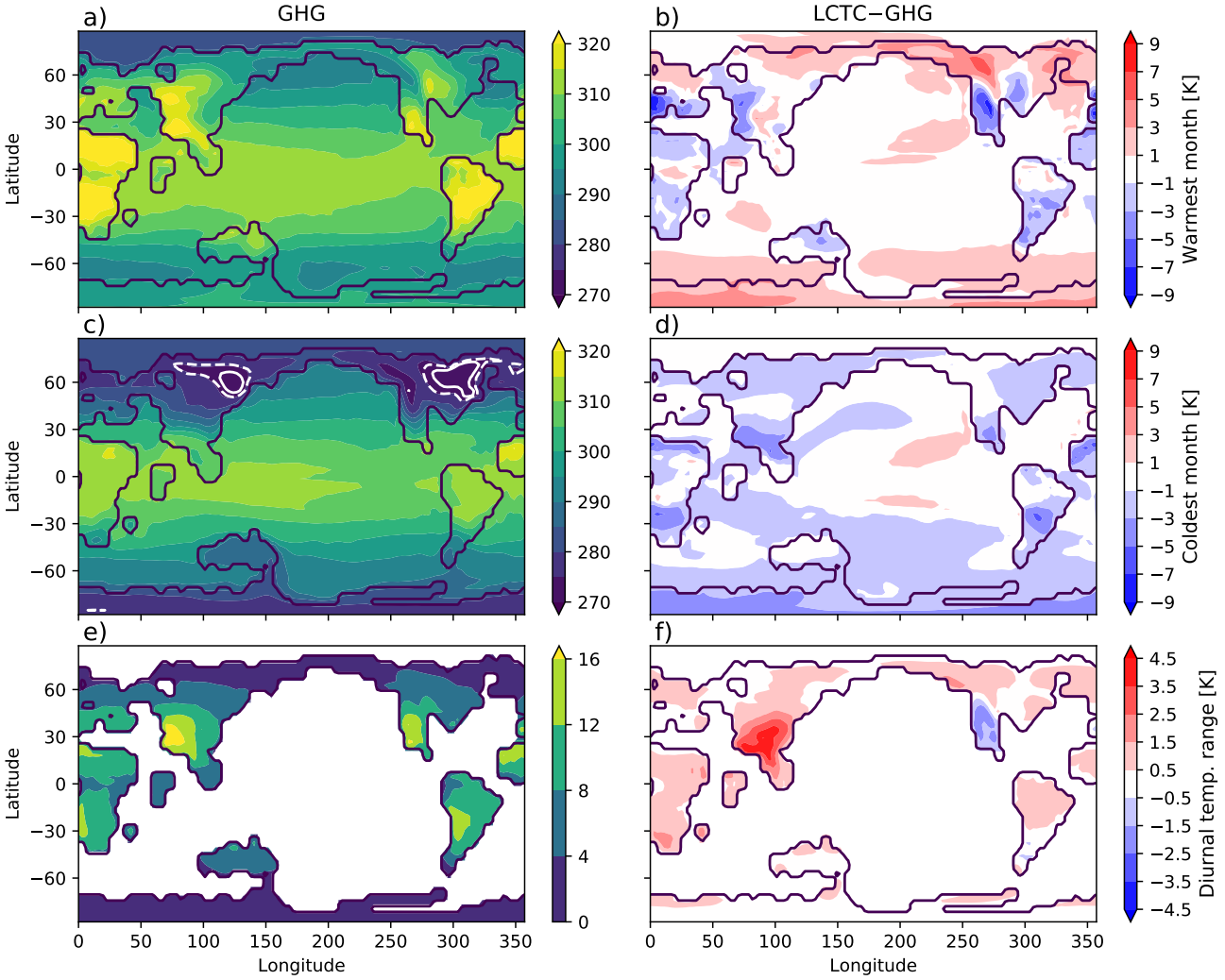

Figure 3. Monthly-mean surface temperature during the warmest month at each grid point in the GHG simulation (a) and its change in the LCTC simulation (b). (c,d) Same as in (a,b) but for the coldest month. (e) Annual-mean diurnal range in surface temperature, defined as the difference between daily maxima and minima, and (f) its change in the LCTC case. White lines in (c) indicate the zero-Celsius contour in the GHG case (solid) and the LCTC case (dashed).

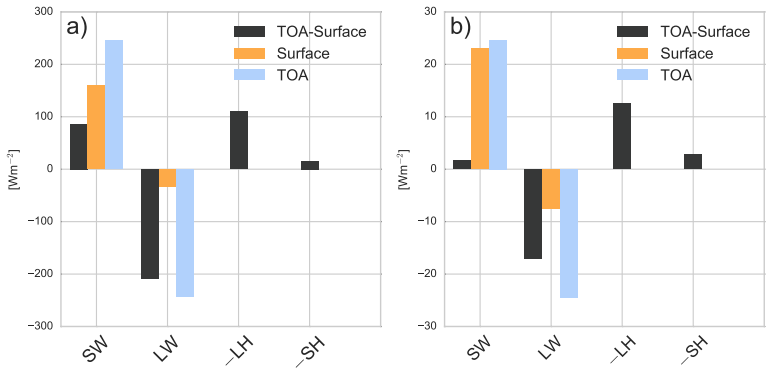

Figure 4. Terms in the global-mean atmospheric energy budget (Equation 1) for (a) the **GHG** simulation and (b) change in the LCTC case (LCTC − **GHG**). **The black bars are the atmospheric heating for both cases.**

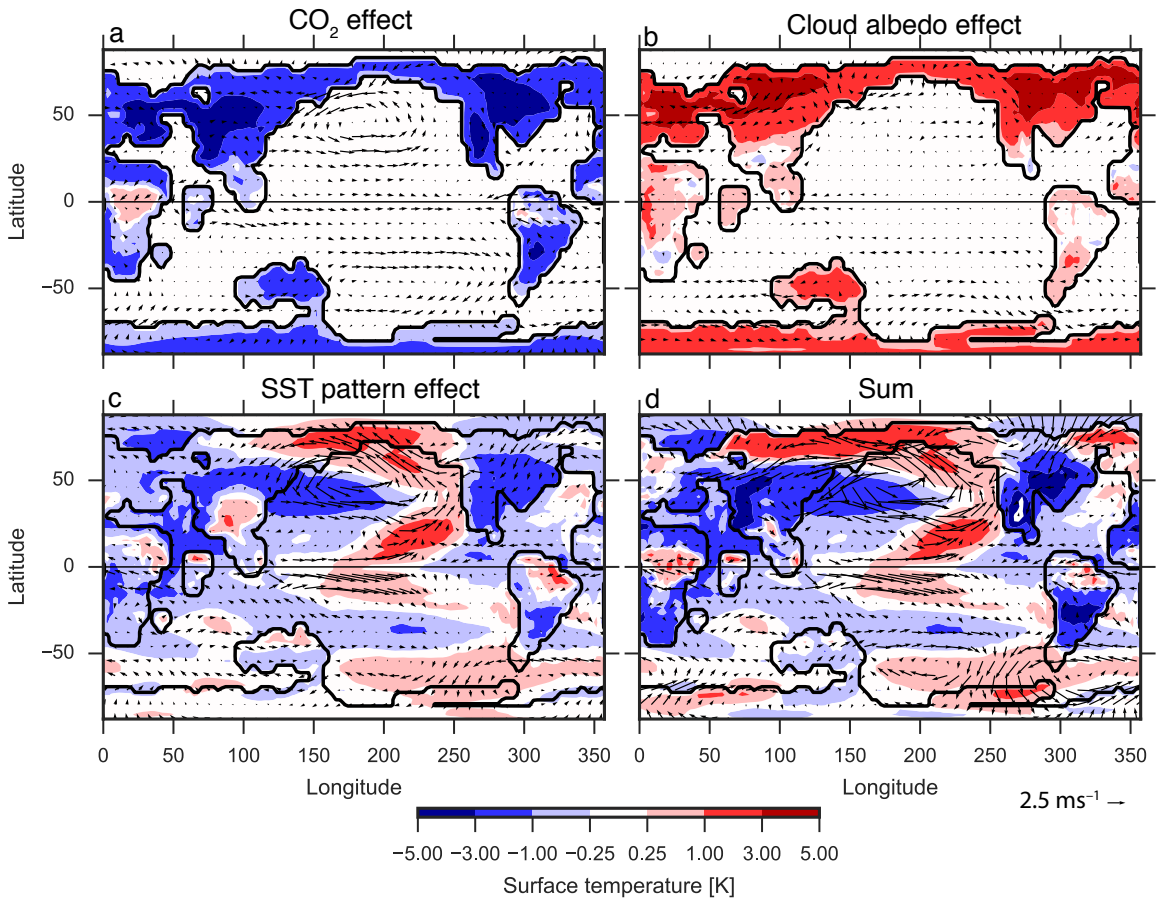

Figure 5. Change in annual-mean surface temperature (shading) and 900 hPa wind (arrows) between the **GHG** run and the fixed SST simulation with (a) reduced CO_2, (b) reduced cloud albedo and (c) change is SST pattern, as well as (d) the sum of all changes.

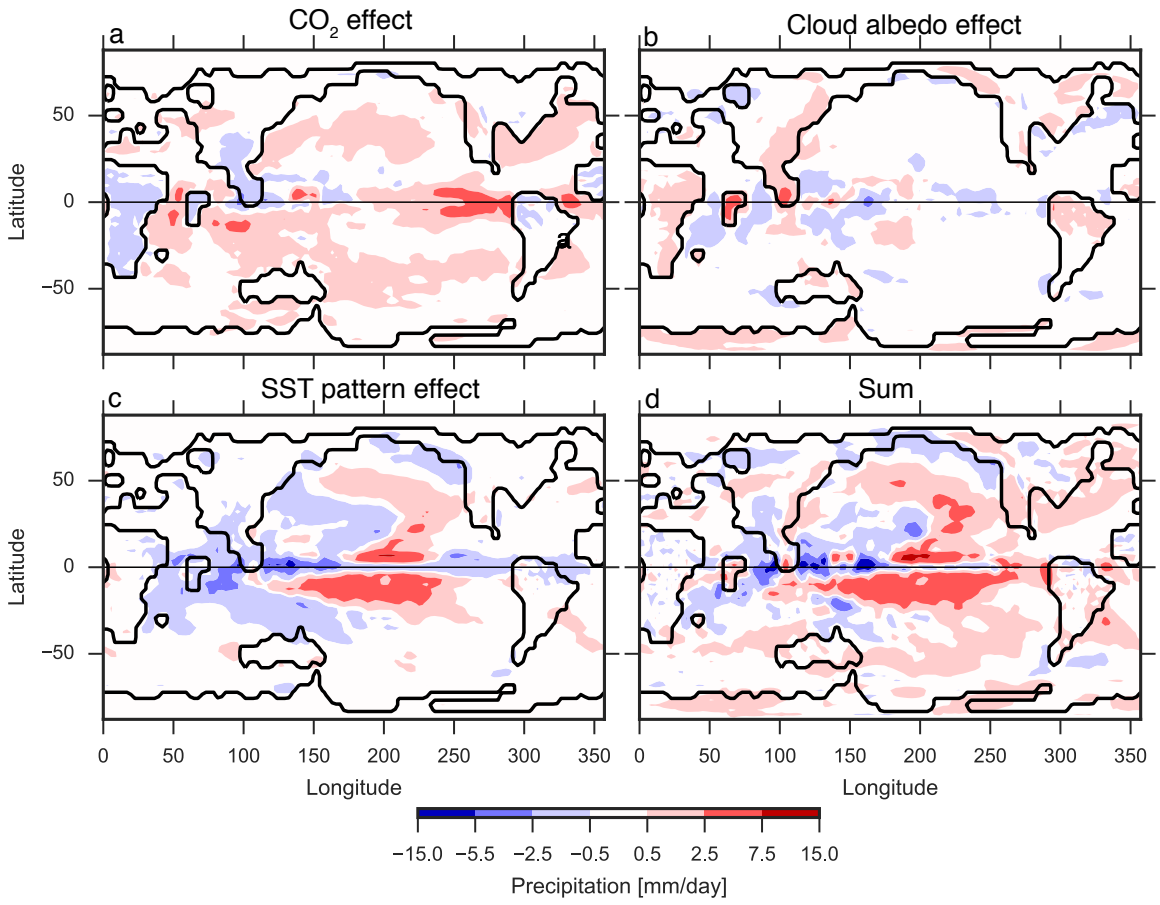

Figure 6. As in Figure 5 but for annual-mean precipitation.

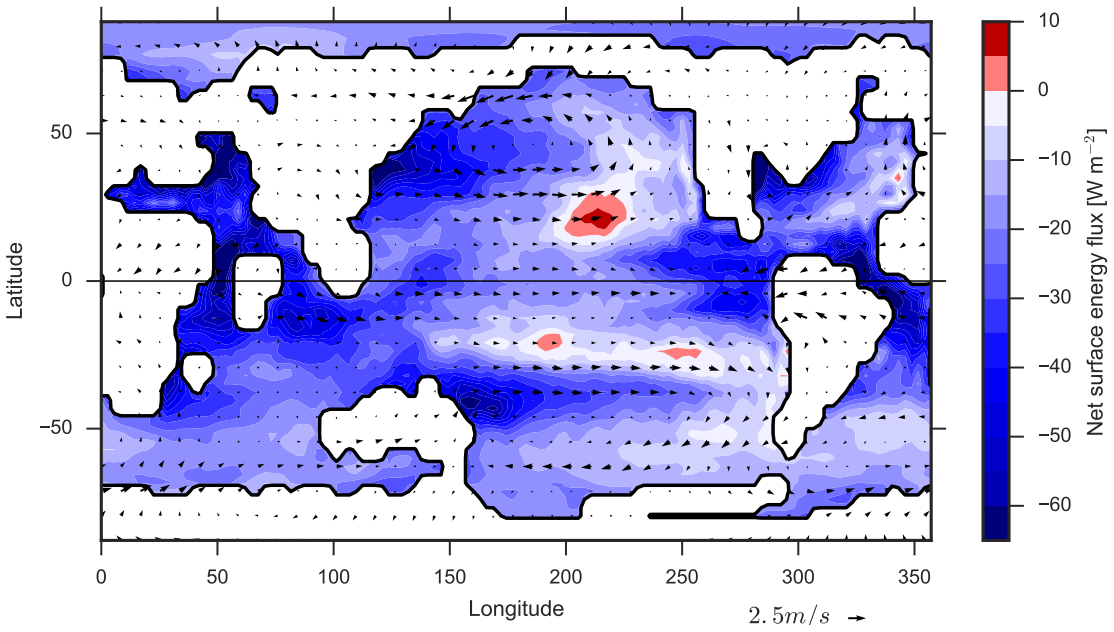

Figure 7. Change in annual-mean net surface energy flux (shading, defined positive downwards) and 900 hPa wind (arrows) between the **GHG** run and the fixed SST run with reduced CO_2.